THE JOURNAL OF BIOLOGICAL CHEMISTRY
Vol. 271, No. 37, Issue of September 13, pp. 22453–22461, 1996
Printed in U.S.A.
© 1996 by The American Society for Biochemistry and Molecular Biology, Inc.

Characterization of Green Alga, Yeast, and Human Centrins

SPECIFIC SUBDOMAIN FEATURES DETERMINE FUNCTIONAL DIVERSITY*

(Received for publication, April 16, 1996, and in revised form, June 29, 1996)

Hans Wiech‡§, Birgitta M. Geier‡§, Thilo Paschke‡, Anne Spang‡, Katrin Grein‡, Jutta Steinkötter¶, Michael Melkonian¶, and Elmar Schiebel‡‖

From the ‡Max-Planck-Institut für Biochemie, Genzentrum, Am Klopferspitz 18a, 82152 Martinsried and the ¶Universität zu Köln, Botanisches Institut, Gyrhofstrasse 15, 50931 Köln, Federal Republic of Germany

Centrins are a subfamily within the superfamily of Ca^{2+}-modulated proteins that play a fundamental role in centrosome duplication and contraction of centrin-based fiber systems. We examined the individual molecular properties of yeast, green alga, and human centrins. Circular dichroism spectroscopy revealed a divergent influence of Ca^{2+} binding on the α-helical content of these proteins. Ca^{2+}-free centrins were elongated in shape as determined by size exclusion chromatography. The presence of Ca^{2+} and binding peptide resulted in more spherical shaped centrins. In contrast to yeast calmodulin, centrins formed multimers in the Ca^{2+}-bound state. This oligomerization was significantly reduced in the absence of Ca^{2+} and in the presence of binding peptide. The Ca^{2+}-dependent polymerization of the green alga *Scherffelia dubia* centrin (SdCen) resulted in a filamentous network. This molecular property was mainly dependent on the amino-terminal subdomain and the peptide-binding site of SdCen. Finally, we analyzed whether SdCen and Cdc31p-SdCen hybrid proteins functionally substitute for the *Saccharomyces cerevisiae* centrin Cdc31p. Only hybrid proteins containing the amino-terminal subdomain or the third EF-hand of SdCen and the other subdomains from Cdc31p were functional *in vivo*.

The microtubule-organizing center organizes the number, direction, and polarity of microtubules in eukaryotic cells. Microtubule-organizing centers differ in appearance from species to species and are known as the centrosome, basal body, or spindle pole body (SPB)[1] (for review, see Refs. 1–3). Besides γ-tubulin (4, 5), members of the centrin protein family are associated with many microtubule-organizing centers in phylogenetically diverse organisms (6). These include algae and protists (7, 8), higher plants (9), yeast (10, 11), and mammals (12, 13). Comparative analysis of centrin protein sequences revealed that they are a closely related family within the larger superfamily of Ca^{2+}-modulated proteins (for review, see Ref. 14). This superfamily includes calmodulin, troponin C, parvalbumin, S-100 protein, myosin light chain, and vitamin D-dependent Ca^{2+}-binding protein (13, 15, 16). In general, centrins are acidic centrosomal or contractile fiber-associated proteins of ~20 kDa that contain four helix-loop-helix subdomains, the so-called EF-hands, which represent potential Ca^{2+}-binding sites.

The amino-terminal subdomain is the most distinctive and variable region of centrins (see Fig. 1). It is about two or three times as long as the corresponding subdomain of related EF-hand proteins such as *Saccharomyces cerevisiae* calmodulin. It has been suggested that the amino-terminal subdomain of centrins confers their functional diversity (17, 18). The EF-hands of centrins are in exact sequence register with those found in calmodulin (see Fig. 1). Due to their high homology and identical domain architecture, the tertiary structure of centrins may be similar to that of calmodulins. Whereas for centrins no three-dimensional structural data are available so far, the crystal structure of Ca^{2+}-coordinated (holo) vertebrate calmodulin revealed a dumbbell-shaped protein with two globular domains, each composed of two EF-hands (for review, see Ref. 19). The two globular domains were connected in *trans* configuration by a long extended central α-helix (20). NMR spectroscopy studies of the Ca^{2+}-bound calmodulin indicated that the central helix is highly mobile in solution and acts as a flexible linker (21, 22).

In green algae, such as *Chlamydomonas reinhardtii* and *Scherffelia dubia*, centrin participates in the contraction of fibers of the nucleus-basal body connectors and of fibers interconnecting the basal bodies (23–25). Centrin is a major component of these fibers, and binding of Ca^{2+} to centrin causes shortening of the fibers even in the absence of ATP. This fiber contraction also plays a fundamental role in microtubule severing at the time of flagella excision in *Chlamydomonas* (26). The centrin-based contraction mechanism is different from the sliding filament mechanism of muscle contraction: the centrin-containing fibers twist and supercoil to form electron-dense globules as they contract (27). *C. reinhardtii* centrin (CrCen) has been studied biochemically after purification from *C. reinhardtii* (15) and after high level expression from *Escherichia coli* (28). CrCen has four Ca^{2+}-binding sites, two with higher and two with lower affinity (28).

In *S. cerevisiae*, centrin is encoded by the essential *CDC31* gene (11, 29). Temperature-sensitive mutants of *CDC31* are defective in the first step of SPB duplication, the formation of the satellite that is assumed to be a precursor of newly formed SPB (30). The phenotype of *cdc31* mutants and the localization of Cdc31p at exactly the site where SPB duplication occurs suggest that Cdc31p plays an important role in the cell cycle-dependent initiation of SPB duplication (10, 29). Cdc31p binds to a short amino acid sequence within the central portion of the SPB component Kar1p (31, 32). Kar1p is associated with the

* This work was supported by Deutsche Forschungsgemeinschaft Grants Schi-295/2-1 and Me-658/9-3. The costs of publication of this article were defrayed in part by the payment of page charges. This article must therefore be hereby marked "*advertisement*" in accordance with 18 U.S.C. Section 1734 solely to indicate this fact.

§ Contributed equally to this work.

‖ To whom correspondence should be addressed. Tel.: 49-89-85783969; Fax: 49-89-85783810; E-mail: eschiebel@genmic.mpg.de.

[1] The abbreviations used are: SPB, spindle pole body; CrCen, *C. reinhardtii* centrin; SdCen, *S. dubia* centrin; HsCen1, *H. sapiens* centrin; HsCen2, *H. sapiens* caltractin; ScCaM, *S. cerevisiae* calmodulin; PCR, polymerase chain reaction; PAGE, polyacrylamide gel electrophoresis; DTT, 1,4-dithiothreitol; MOPS, 4-morpholinepropanesulfonic acid; AMM, apparent molecular mass.

Downloaded from http://www.jbc.org/ at Universitaetsbibliothek Medizin on November 16, 2017

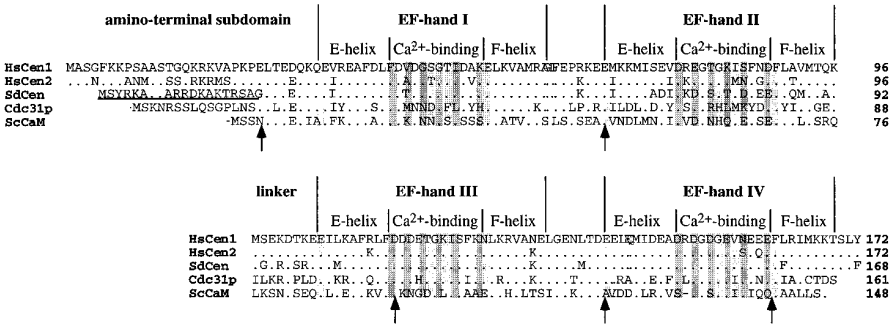

FIG. 1. **Sequence alignment of centrins and ScCaM.** The amino acid sequences of HsCen1 (13), HsCen2 (12), SdCen (17), Cdc31p (11, 29), and ScCaM (39) are aligned. Centrins are divided into an amino-terminal subdomain, EF-hands I and II (which are separated from EF-hands III and IV by a short linker region), and the carboxyl-terminal subdomain. Each EF-hand consists of an E-helix, the Ca^{2+}-binding site, and an F-helix. *Light gray* amino acids indicate conserved residues within the EF-hands, whereas *dark gray* amino acids are involved in Ca^{2+} coordination. The *underlined* amino acid sequence of SdCen was synthesized and used for competition experiments (see Fig. 7*A*). The *arrows* indicate the fusion sites of Cdc31p-SdCen and Cdc31p-ScCaM hybrid proteins (see Figs. 7*A* and 8).

same SPB substructure as Cdc31p (29, 32) and is the only known structural component that interacts with a centrin. Cdc31p binding to Kar1p is not absolutely required for SPB duplication since certain mutations in *CDC31* suppress the deletion of the normally essential *KAR1* gene (33). The cloning of human centrins has unexpectedly revealed two highly related isogenes (12, 13). Immunofluorescence experiments have indicated that they may be associated with centrioles (13) or with the pericentriolar material (12).

In this paper, we provide the first comparative biochemical analysis of the centrins from *S. cerevisiae* (Cdc31p), *S. dubia* (SdCen), *Homo sapiens* (HsCen1 and HsCen2), and *S. cerevisiae* calmodulin (ScCaM). Their biochemical and biophysical properties were analyzed under standard conditions in order to achieve comparable data. In addition, we investigated whether SdCen and Cdc31p-SdCen hybrid proteins can functionally replace Cdc31p *in vivo*. We have obtained evidence that centrins and ScCaM differ in their Ca^{2+}-dependent properties and that centrins show a remarkable biochemical divergence.

EXPERIMENTAL PROCEDURES

Media, Bacterial and Yeast Transformation, and DNA Techniques—Media for growth of yeast were prepared as described (34). Yeast and *E. coli* cells were transformed according to published protocols (35, 36). The nucleotide sequence of all PCR constructs was determined by the chain termination method (37). All other DNA manipulations were performed as described (38).

Construction of Plasmids—Plasmids are listed in Table I. *CMD1* (39), *CDC31* (11), *HsCEN1* (13), *HsCEN2* (12), and *SdCEN* (17) were amplified by PCR using plasmids pSM61 (32), pSM14 (29), pSK333A, AG24 and pKsdCen, respectively, as templates. The sense primers were designed such that the translation initiation codon (ATG) of the five genes formed part of a *Nde*I restriction site. The antisense primers were located ~50 nucleotides downstream of the stop codon and introduced an *Eco*RI or a *Pst*I restriction site. The PCR products were subcloned into the expression vector pT7-7 (40).

Construction of CDC31-SdCEN Gene Fusions—The sites of gene fusion are indicated in Fig. 1 (*arrows*). *CDC31-SdCEN* gene fusions were constructed by recombinant PCR. All gene fusions carried the promoter and the terminator regions of *CDC31* (11). Primers CDC31-I (5′-TAACCCAAAGCTTGATGTATTTCTCTCTAGTA-3′) and CDC31-B (5′-TAACCCAGAGCTCGCTCGAAATGGCTATTGAACTCTAG-3′), carrying a *Hin*dIII and a *Sac*I restriction site (underlined), respectively, were used for the subcloning of the PCR products into the yeast *E. coli* shuttle vector pRS425 or pRS426 (41). The *CDC31*$^{3\text{-}CMD1}$ gene fusion was constructed similarly.

CDC31 and SdCEN under the Control of the GAL1 Promoter—*CDC31* was amplified by PCR. The sense primer CDC31-*Bam*HI introduced a *Bam*HI restriction site just upstream of the ATG start codon of *CDC31*. The PCR product was subcloned into the yeast expression vector pYES2 (Invitrogen) to give plasmid pSM59. *SdCEN* and *SdCEN*$^{N\text{-}CDC31}$ were subcloned in a similar manner into pYES2 to give pAH2 and pSM102, respectively.

Functionality and Expression of the CDC31-SdCEN Gene Fusions—To test whether *SdCEN* and *CDC31-SdCEN* are functional in yeast, we constructed ESM109 (Δ*cdc31::HIS3* pSM85), which has a disruption of the chromosomal *CDC31* gene and is maintained by *CDC31* on a *URA3*-based plasmid (pSM85). ESM109 did not grow on plates of 5-fluoroorotic acid, which selects against the *URA3* plasmid, showing that *CDC31* is essential for growth (29). However, ESM109 grew on 5-fluoroorotic acid when a second *CDC31* gene was provided on the *LEU2*-based plasmid pRS425-*CDC31* (pSM234). This property of ESM109 was used to test whether *CDC31-SdCEN* gene fusions on plasmid pRS425 provided *CDC31* function.

Alternatively, strain ESM56 (32) was used for the complementation test. Strain ESM56 carries *CDC31* under the control of the *MET3* promoter (42) integrated into the *LEU2* locus. The chromosomal *CDC31* gene is disrupted by the *HIS3* gene. ESM56 cells grow at a normal rate on minimal medium without methionine. The addition of methionine to the growth medium represses *CDC31* expression from the *MET3* promoter, causing cell cycle arrest after Cdc31p depletion. The presence of an additional copy of *CDC31* under the control of its own promoter restored growth on plates containing methionine. This property of ESM56 was used to test the functionality of *CDC31-SdCEN* gene fusions. ESM56 was transformed with plasmids pSM144 and pSM155 to pSM159 (Table I), with selection being made on synthetic minimal plates containing adenine, lysine, and tryptophan (SM+ALT). Growth on the repressing synthetic complete plates containing 2 mM methionine (SC+Met) indicated that the *CDC31-SdCEN* gene fusion on plasmid pRS426 provided *CDC31* function.

The functionality of *GAL1-SdCEN* or *GAL1-SdCEN*$^{N\text{-}CDC31}$ in pYES2 was tested after transformation in ESM56 by growth on SC+Met medium containing either 2% glucose (repression of the *GAL1* promoter) or 2% galactose/raffinose (induction of the *GAL1* promoter). Plasmid pSM59 (*GAL1-CDC31*) was used as a positive control, and plasmid pYES2 (*GAL1* promoter) was used as a negative control.

The expression of *CDC31-SdCEN* gene fusions from the *CDC31* promoter was tested in ESM56. ESM56 cells carrying *CDC31-SdCEN* on plasmid pRS426 were grown on SM+ALT medium at 30 °C overnight. The cultures were then diluted 1:10 with SC+Met or SM+ALT medium. Cells were incubated for 6 h at 30 °C. Cell extracts were prepared as described (43). Protein extracts (80 μg of protein) (44) were separated by SDS-PAGE and then transferred onto nitrocellulose membranes. Cdc31p-SdCen fusion proteins were detected with antibodies against Cdc31p (29). The Cdc31p signal in ESM56 cells grown in the presence of methionine reflects the steady-state level of plasmid-encoded Cdc31p-SdCen fusion proteins. The signals of cells grown on SM+ALT medium are the sum of *MET3-CDC31* and plasmid-encoded *CDC31-SdCEN*.

Protein Purification—TY medium (5 g of NaCl, 5 g of yeast extract, 10 g of Bacto-tryptone/liter) (36 liters; 100 μg/ml ampicillin) was inoculated with *E. coli* BL21(DE3) cells carrying centrins or calmodulin genes in expression vector pT7-7. Cells were incubated at 37 °C to an absorbance at 600 nm of 0.4. Isopropyl-β-D-thiogalactopyranoside (0.5 mM) was added for 2 h at 30 °C to induce the synthesis of the recombinant proteins. The cell pellet was washed with 400 ml of wash buffer (25 mM Tris, 17 mM HCl, 400 mM NaCl, 2 mM $CaCl_2$, 5% glycerol, 5 mM DTT, 2.5 mM phenylmethylsulfonyl fluoride, and 2.5 mM *p*-aminobenzamidine). Cells were resuspended in 360 ml of lysis buffer (50 mM Tris, 34

Downloaded from http://www.jbc.org/ at Universitaetsbibliothek Medizin on November 16, 2017

TABLE I
Plasmids

Plasmid	Construction	Source
AG24	*HsCEN2*	M. Bornens
pAH2	*SdCEN* in pYES2: *GAL1-SdCEN*	This study
pKSdCen	*SdCEN*	Ref. 17
pRS425	2 μm, *LEU2*-based yeast *E. coli* shuttle vector	Ref. 41
pRS426	2 μm, *URA3*-based yeast *E. coli* shuttle vector	Ref. 41
pSK333A	*HsCEN1*	Ref. 13
pSM5	*CDC31* in pT7–7	Ref. 29
pSM14	*CDC31* in pBluescript SK	Ref. 29
pSM56	*CDC31* in pRS426	This study
pSM59	*CDC31* in pYES2: *GAL1-CDC31*	This study
pSM61	*CMD1* in pUC18	Ref. 32
pSM71	*CMD1* in pT7–7	Ref. 32
pSM85	Yeast *E. coli* shuttle vector carrying *URA3 ADE3 CDC31*	This study
pSM102	$SdCEN^{N\text{-}CDC31}$ in pYES2: $GAL1\text{-}SdCEN^{N\text{-}CDC31}$	This study
pSM144	$CDC31^{N\text{-}SdCEN}$ in pRS426	This study
pSM155	$CDC31^{1\text{-}SdCEN}$ in pRS426	This study
pSM156	$CDC31^{2\text{-}SdCEN}$ in pRS426	This study
pSM157	$CDC31^{3\text{-}SdCEN}$ in pRS426	This study
pSM158	$CDC31^{4\text{-}SdCEN}$ in pRS426	This study
pSM159	$CDC31^{C\text{-}SdCEN}$ in pRS426	This study
pSM160	$CDC31^{N\text{-}SdCEN}$ in pRS425	This study
pSM161	$CDC31^{1\text{-}SdCEN}$ in pRS425	This study
pSM162	$CDC31^{2\text{-}SdCEN}$ in pRS425	This study
pSM163	$CDC31^{3\text{-}SdCEN}$ in pRS425	This study
pSM164	$CDC31^{4\text{-}SdCEN}$ in pRS425	This study
pSM165	$CDC31^{C\text{-}SdCEN}$ in pRS425	This study
pSM169	*SdCEN* in pT7–7	This study
pSM170	$CDC31^{N\text{-}SdCEN}$ in pT7–7	This study
pSM234	*CDC31* in pRS425	This study
pSM248	*HsCEN1* in pT7–7	This study
pSM293	$CDC31^{3\text{-}CMD1}$ in pRS426	This study
pSM308	$SdCEN^{N\text{-}CDC31}$ in pT7–7	This study
pT7–7	Phage T7 promoter	Ref. 40
pTP6	*HsCEN2* in pT7–7	This study
pYES2	2 μm, *URA3*-based yeast *E. coli* shuttle vector *GAL1* promoter	Invitrogen

mM HCl, 2 mM $CaCl_2$, 0.005% Triton X-100, 1 mM EDTA, 4 mM DTT, 2 mM phenylmethylsulfonyl fluoride, and 2 mM *p*-aminobenzamidine) and lyzed by sonication. The lysate was centrifuged at 16,000 × *g* for 15 min at 4 °C. The supernatant was collected, and the pellet was re-extracted as described above. The pooled supernatants were supplemented with 2 mM DTT, 1 mM phenylmethylsulfonyl fluoride, and 1 mM *p*-aminobenzamidine and incubated in a boiling water bath until the solution reached 80 °C. The solution was cooled in a CO_2/ethanol bath to 10 °C. Denatured proteins were removed by centrifugation. All following chromatography steps were performed at 4 °C.

The supernatant was incubated with 150 ml of DEAE-cellulose (Sigma) equilibrated with AEC buffer (50 mM Tris, 34 mM HCl, and 1 mM DTT) for 2 h. After washing the DEAE-cellulose with 350 ml of AEC buffer, a linear gradient (total volume of 1 liter) from 0 to 1 M NaCl in AEC buffer was applied. Fractions eluting from 100 to 350 mM NaCl were pooled; adjusted to a final concentration of 1.5 M NaCl, 5 mM $CaCl_2$, and 13% glycerol; and applied to a 75-ml phenyl-Sepharose HP column (Pharmacia Biotech Inc.) equilibrated with HIC buffer (50 mM Tris, 34 mM HCl, 1.5 M NaCl, 5 mM $CaCl_2$, 10% glycerol, and 1 mM DTT). The column was washed with HIC buffer, and bound proteins were eluted with HIC-E buffer (10 mM Tris, 6.8 mM HCl, 5 mM EGTA, 10% glycerol, and 1 mM DTT).

The pooled fractions were concentrated by ultrafiltration (Millipore Corp.) to 2 ml and applied to a Superdex 75 HiLoad 16/60 column (Pharmacia Biotech FPLC system) equilibrated with 50 mM Tris, 34 mM HCl, 100 mM NaCl, 10% glycerol, 1 mM DTT, and 0.5 mM EGTA. Fractions containing the recombinant protein were concentrated to 1.5 mM.

Analytical Techniques—Protein concentration was determined using bovine serum albumin as a standard (45). Alternatively, the molar extinction coefficient was used to calculate the concentration. We determined the molar extinction coefficient at λ = 276 nm of Cdc31p (18,751 Da) to be 7250 $M^{-1}\,cm^{-1}$ based on a mixture of five tyrosine and nine phenylalanine residues measured in the presence or absence of 6 M guanidium hydrochloride. The concentration of peptides was determined using the tryptophan absorbance at λ = 280 nm.

CD Spectroscopy—CD measurements were performed using a Jobin Yvon Mark IVCD spectrometer. Measurements using 0.1 mg/ml protein were first recorded in 10 mM MOPS, 5 mM KOH, 50 mM KCl, and 0.5 mM EGTA at 20 °C in a 10-mm path cuvette. Ca^{2+} (2 mM) was added, followed by a second recording. The average of 10 spectra from 198 to 240 nm with 0.1-nm spacing was used for the calculations of α-helical content with the CD package of CONTIN (46). The α-helical contents are means of at least four independent experiments.

Determination of the Apparent Molecular Masses of Centrins and ScCaM—The apparent molecular mass (AMM) was determined by size exclusion chromatography (Superdex 75 PC 3.2/30 column, Pharmacia Biotech Smart System). The column was calibrated with globular proteins (bovine serum albumin (66 kDa; K_D = 0.123), egg albumin (45 kDa; K_D = 0.176), carbonic anhydrase (29 kDa; K_D = 0.262), and RNase A (13.7 kDa; K_D = 0.384)) at a flow rate of 6.25 mm/min at 20 °C with 10 mM MOPS, 5 mM KOH, 100 mM NaCl, and 1 mM DTT in the absence (0.5 mM EGTA) or presence of 0.1 mM Ca^{2+}. Blue dextran was used to determine the void volume (V_0 = 878 μl), and acetone to estimate the pore volume (V_P = 1525 μl). The distribution coefficient (K_D) was calculated using the equation $K_D = {V_P}^{-1}(V_R - V_0)$, where V_R is the retention volume. The AMMs were determined with the equation AMM = 133.33 $e^{(-5.9155\ K_D)}$ (r = 0.9976). In some experiments, the EF-hand proteins were preincubated with a 4-fold molar excess of Kar1p peptide (KKRELIESKWHRLLFHDKK; centrins) or Spc110p peptide (RRLSFKTVAWLVLASVRMKRI; ScCaM) for 10 min at 20 °C. The Spc110p peptide contains a Leu to Trp exchange at position 10, which does not influence the binding properties. All peptides were synthesized by the Max-Planck-Institut Peptide Service.

Association Studies—Centrins and ScCaM were incubated at a protein concentration of 1.5 mM with 10 mM Ca^{2+} in P buffer (50 mM Tris, 34 mM HCl, 100 mM NaCl, 10% glycerol, and 1 mM DTT). For the inhibition of SdCen polymerization by peptides, a 4-fold molar excess of Kar1p peptide, a peptide corresponding to the 20 amino acids of the amino-terminal subdomain of SdCen (MSYRKAASARRDKAKTRSAG) or yeast α-factor (WHWLQLKPQPMY), was incubated with SdCen for 10 min at 20 °C before the addition of 10 mM Ca^{2+}. The samples were centrifuged at 10,000 × *g* for 15 min at 4 °C. The sediment was washed with 10 mM Ca^{2+} in P buffer and centrifuged as described above, and the remaining sediment was washed with 10 mM EGTA in P buffer and finally dissolved in 2% SDS. Fractions were analyzed by SDS-PAGE and densitometry (Howtek Scanmaster 3).

Formation of Filamentous Structures—The polymerization reaction

Downloaded from http://www.jbc.org/ at Universitaetsbibliothek Medizin on November 16, 2017

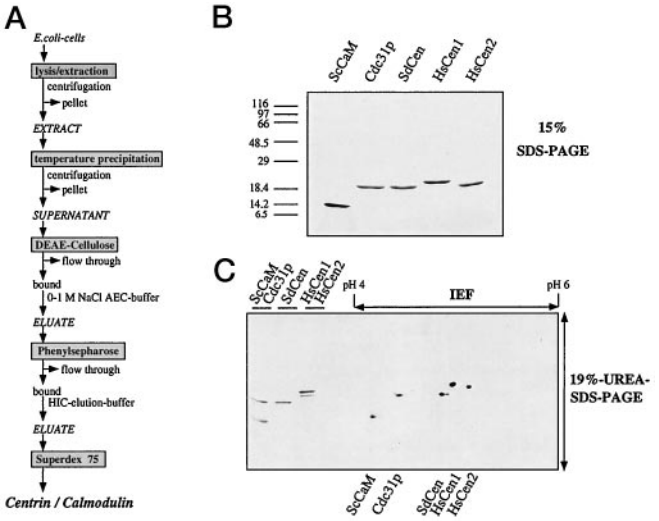

FIG. 2. **Purification scheme and analysis of the purified EF-hand proteins by gel electrophoresis.** *A*, flow diagram of the purification of centrins and ScCaM. *B*, analysis of the purified centrins and calmodulin. Purified proteins (1 μg each) were analyzed on a 15% SDS-polyacrylamide gel. The gel was stained with Coomassie Blue G. Molecular mass standards were β-galactosidase, phosphorylase *b*, bovine serum albumin, fumarase, carbonic anhydrase, β-lactalbumin, α-lactalbumin, and aprotinin. *C*, estimation of the isoelectric point (*IEF*) values of centrins and ScCaM. A mixture of purified ScCaM, Cdc31p, SdCen, HsCen1, and HsCen2 was analyzed by isoelectric focusing using a linear immobilized pH gradient from pH 4 to 6. This gel was then layered on top of a 19% Tris/urea-SDS-polyacrylamide gel. Electrophoresis was performed simultaneously with 1 μg of ScCaM, Cdc31p, SdCen, HsCen1, and HsCen2. The gel was stained with Coomassie Blue G. The pI values of ScCaM, Cdc31p, SdCen1, HsCen1, and HsCen2 were 4.32, 4.51, 4.85, 4.92, and 5.05, respectively. These determined pI values were 0.25 pH units above the calculated values.

was induced on a nickel grid coated with Formvar (placed in the slot of a multichamber dialysis apparatus) with a gradient from 0 to 1 mM Ca^{2+} in P buffer over 3 h at 20 °C. The grids were washed with 1 mM Ca^{2+} or 10 mM EGTA in P buffer. The samples were prepared for electron microscopy using a positive staining procedure. Grids were incubated with lead citrate, washed with H_2O, and than stained with 2% uranyl acetate in 70% methanol. Finally, the grids were washed with 70% methanol and incubated again with lead citrate.

RESULTS

Purification of ScCaM, Cdc31p, SdCen, HsCen1, and HsCen2—The strategy (Fig. 2*A*) for the purification of ScCaM, Cdc31p, SdCen, HsCen1, and HsCen2 is based on published protocols (28, 29, 47, 48); however, it was optimized to achieve purification of all five EF-hand proteins under identical conditions. We obtained ~100 mg of pure protein from 36 liters of *E. coli* culture after a 35-fold enrichment, with a yield of 40%. All proteins were at least 99% pure as judged by one- and two-dimensional gel electrophoresis (Fig. 2, *B* and *C*) as well as by the absence of tryptophan fluorescence. The latter could be used as purity criteria since centrins and ScCaM do not contain intrinsic tryptophan residues. We conclude that our protocol is suitable for the purification of four centrins and ScCaM, suggesting that it may also be useful for the purification of other EF-hand proteins.

Ca^{2+}-induced Conformational Changes—Analysis of the EF-hand protein spectrin revealed that EF-hands change their conformation upon Ca^{2+} binding (49). Therefore, we investigated by CD spectroscopy and size exclusion chromatography whether Ca^{2+} binding to centrins induces conformational changes. The CD spectra were first recorded for the Ca^{2+}-free apo form of the proteins. Ca^{2+} was then added to obtain the holo forms, which were analyzed by a second CD recording (Fig. 3). The α-helical values were calculated, with 69% for ScCaM,

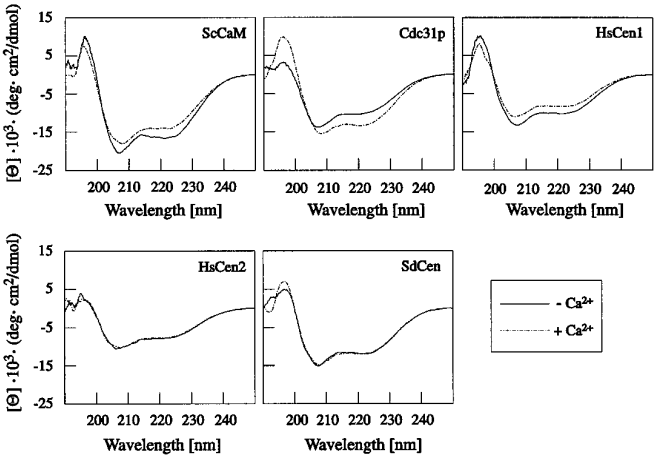

FIG. 3. **Circular dichroism spectra of the apo and holo forms of ScCaM and centrins.** The CD spectra were recorded at a protein concentration of 0.1 mg/ml at 20 °C in the presence of EGTA ($-Ca^{2+}$) or after the addition of $CaCl_2$ ($+Ca^{2+}$).

42% for Cdc31p, 50% for SdCen, 37% for HsCen1, and 42% for HsCen2. A decrease in α-helical content upon Ca^{2+} binding was measured for ScCaM (10%) and HsCen1 (12%), while Cdc31p showed an increase by 12% (Fig. 3). No change in α-helical content was observed for HsCen2 and SdCen, which does not exclude Ca^{2+}-induced conformational changes. However, it indicates that the sum of the structural elements contributing to the CD spectrum remained constant.

Conformational changes accompanied by an alteration in molecular shape are detectable by size exclusion chromatography as a change in the AMM. Such studies require a highly reproducible size exclusion chromatography system. Using standardized conditions, we could measure the AMMs of centrins with an accuracy of ±0.2 kDa. At a protein concentration at or below 10 μM, all apo forms of the four centrins and ScCaM revealed an AMM that was ~1.7-fold higher than the calculated molecular mass (Table II). It is known that vertebrate calmodulin resembles an elongated molecule (21, 22) and that the long axis of the molecule causes a defined overestimation of the AMM when globular proteins are used for column calibration (28). Considering the homology between calmodulins and centrins, it is most likely that centrins are also elongated molecules, explaining their behavior on sizing columns.

We determined the AMMs of centrins and ScCaM in their Ca^{2+}-bound state (holo form, Table II). Since comparison of the holo and apo forms may indicate conformational changes, we expressed the relative AMM (ratio of the holo to apo forms) in Fig. 4*A*. The *horizontal line* at 1.0 indicates the relative AMM of the apo forms. While the relative AMM increased for ScCaM (Fig. 4*A*, indicated by the *bar* above the *horizontal line*), it decreased for all centrins (indicated by the *bars* below the *horizontal line*). Within the centrin family, the relative Ca^{2+}-induced change was lowest for HsCen2, followed by HsCen1 and Cdc31p, and was most pronounced for SdCen (Fig. 4*A*). These alterations were specific for Ca^{2+} since Mg^{2+} did not influence the AMM (data not shown). Since the alterations in the AMM are likely the result of conformational changes (see "Discussion"), we suggest that centrins and calmodulins are differently influenced by Ca^{2+} binding, resulting in a more extended conformation for ScCaM and a more compact one for centrins. Interestingly, centrins bound in the presence of Ca^{2+} to the hydrophobic phenyl-Sepharose column and were eluted by the removal of Ca^{2+} (Fig. 2*A*), suggesting that centrins, similar to calmodulins, expose a hydrophobic surface in their more compact Ca^{2+}-bound form.

Influence of Peptide Binding—The four centrins, but not

Downloaded from http://www.jbc.org/ at Universitaetsbibliothek Medizin on November 16, 2017

TABLE II
Determination of the apparent molecular masses of centrins and ScCaM

The calculated molecular mass is based on the deduced amino acid sequences (see Fig. 1). The AMM was determined by size exclusion chromatography with an accuracy of ±0.2 kDa (n = 5). The AMMs of the apo, holo, and peptide-bound holo forms of centrins and ScCaM were analyzed at protein concentrations of 2.5, 5, and 10 μM. The AMM remained constant at these protein concentrations.

Protein	CMM[a]	AMM		
		Apo	Holo	Holo + peptide
	kDa		*kDa*	
ScCaM	16.74	28.2	33.4	24.9
Cdc31p	18.75	33.3	27.8	28.4
SdCen	19.33	32.8	23.1	24.4
HsCen1	19.57	35.3	33.4	29.7
HsCen2	19.74	34.2	33.6	28.8

[a] CCM, calculated molecular mass.

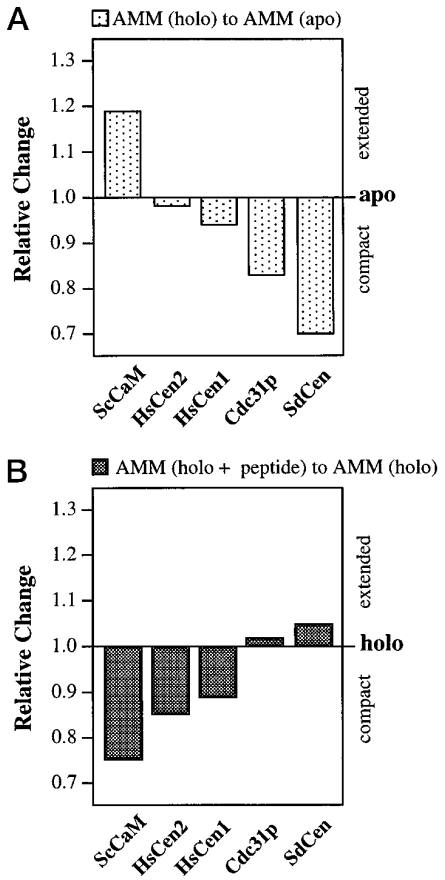

FIG. 4. **Relative change in apparent molecular mass of ScCaM and centrins upon Ca^{2+} and peptide binding.** The AMMs (listed in Table II) of ScCaM and centrins were analyzed by size exclusion chromatography at a protein concentration of 10 μM. The ratios of the AMMs of the holo to apo forms (*A*) (*AMM (holo)/AMM (apo)*) and of the peptide-bound holo to holo forms (*B*) (*AMM (holo + peptide)/AMM (holo)*) are shown.

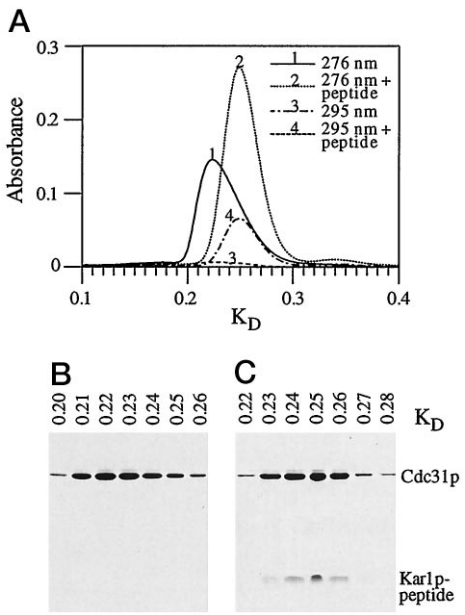

FIG. 5. **Interaction of Cdc31p with Cdc31p-binding peptide of Kar1p.** *A*, Cdc31p (10 μl of a 100 μM solution) in the holo state in the presence (*curves 2* and *4*) or absence (*curves 1* and *3*) of the Kar1p peptide was analyzed by size exclusion chromatography. The distribution coefficient (K_D) is inversely related to the AMM. The absorbances at 276 nm (*curves 1* and *2*) and 295 nm (*curves 3* and *4*) were recorded. At 276 nm, Cdc31p and the Kar1p peptide were detected, and at 295 nm, only the Kar1p peptide was detected. This was due to the absence of tryptophan in Cdc31p, whereas the Kar1p peptide contains this amino acid. Peak fractions of the holo form (*B*) or of the holo form-Kar1p peptide complex (*C*) were analyzed by 19% Tris/urea-SDS-PAGE and stained with Coomassie Blue G.

ScCaM, bind with high affinity to a small peptide corresponding to the Cdc31p-binding site of Kar1p (32).[2] ScCaM, however, interacts with a peptide corresponding to the ScCaM-binding site of the SPB component Spc110p (50, 51, 60). We used these peptides for the further characterization of centrins. As an example of our analysis, the fractionation of Cdc31p with and without the Kar1p peptide by size exclusion chromatography is shown in Fig. 5. The chromatograms were recorded at two wavelengths (276 and 295 nm). This was useful since the Kar1p peptide, but not the centrins, contain the amino acid tryptophan, which is detected by absorbance at 295 nm. Therefore, the 276 nm signal mainly results from Cdc31p, while the 295 nm signal indicates the position of the Kar1p peptide. In this experiment, Cdc31p eluted from the size exclusion column with a distribution coefficient (K_D) of 0.23 (Fig. 5*A*, *curve 1*). The K_D is inversely related to the AMM (see "Experimental Procedures"). The addition of the Kar1p peptide was accompanied by a shift of the Cdc31p signal (276 nm) to a higher K_D and by an increase in absorbance (Fig. 5*A*, compare *curves 1* and *2*). In addition, a tryptophan signal (295 nm) (Fig. 5*A*, compare *curves 3* and *4*) with the same K_D as Cdc31p was observed, suggesting that Cdc31p forms a complex with the peptide. The unbound Kar1p peptide is not seen on the chromatogram since its K_D is above 0.4. Corresponding peak fractions were analyzed by SDS-PAGE, confirming that the Kar1p peptide cofractionated with Cdc31p (Fig. 5, compare *B* (no peptide) with *C* (Cdc31p peptide complex)). No Cdc31p-Kar1p peptide complex was obtained when Cdc31p was in its Ca^{2+}-free apo state, suggesting that binding of the Kar1p peptide to Cdc31p is Ca^{2+}-dependent. Similarly, no Cdc31p peptide complex was observed with control peptides, *e.g.* α-factor (data not shown).

[2] B. M. Geier, H. Wiech, and E. Schiebel, submitted for publication.

Downloaded from http://www.jbc.org/ at Universitaetsbibliothek Medizin on November 16, 2017

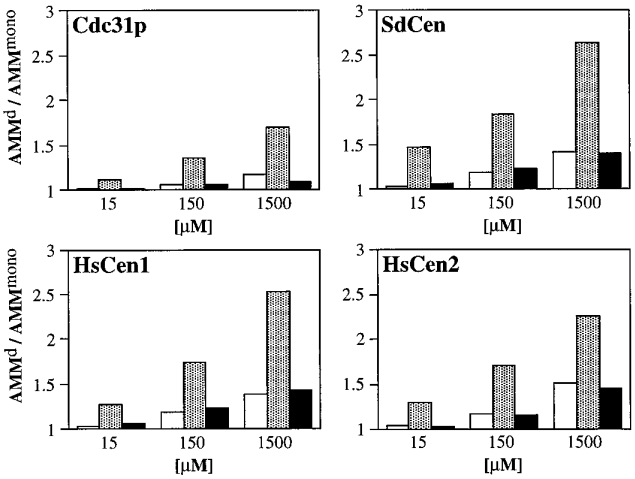

FIG. 6. **Ca^{2+}-, concentration-, and peptide-dependent association of centrins.** The AMM (n = 4) was determined using protein concentrations of 15 μM, 150 μM, or 1.5 mM purified centrins in the absence (*apo*) (*white bars*) or presence of Ca^{2+} ions (*holo*) (*dotted bars*) or the Kar1p peptide (*holo + peptide*) (*black bars*). Shown is the ratio of the AMM (AMM^{d}) at the outlined protein concentrations to the monomeric AMM (AMM^{mono}; AMM at 10 μM concentrations of the apo, holo, and peptide-bound holo forms in Table II).

It has been shown that vertebrate calmodulin adopts a more globular shape after binding to a peptide (21). Based on this finding, we expected that binding of peptide to centrins and ScCaM would result in a decrease in the AMM. The AMMs of the centrin and ScCaM peptide complexes were determined by size exclusion chromatography as described for Fig. 5*A* (Table II) and compared with those of the holo forms (Fig. 4*B*). As expected, binding of peptide caused a decrease in the relative AMMs of ScCaM and the two human centrins. In contrast, a slight increase was observed for Cdc31p and SdCen (Fig. 4*B*). Our results suggest the formation of a more compact structure upon peptide binding for ScCaM and the two human centrins and a more extended conformation for Cdc31p and SdCen.

Ca^{2+}-dependent Formation of Polymers—Centrin is the major component of the contractile filament system in green algae (24, 52). Therefore, we studied the polymerization capability of the different centrins and ScCaM. Increasing concentrations of ScCaM and the four centrins were analyzed by size exclusion chromatography. ScCaM was monomeric even at protein concentrations up to 1.5 mM and at Ca^{2+} concentrations of 10 mM (data not shown). However, centrins formed multimers in the holo state above a protein concentration of 10 μM (Fig. 6, *holo*). The formation of multimeric structures was strongly reduced by peptide (Fig. 6, *holo + peptide*) or by the removal of Ca^{2+} (Fig. 6, *apo*). In summary, a clear difference between ScCaM and centrins is the tendency of centrins to form multimers.

SdCen Forms Filamentous Networks—We investigated the properties and the extent of centrin polymers. The four centrins were incubated at a protein concentration of 1.5 mM and with a 100-fold higher Ca^{2+} concentration (10 mM) as in Fig. 6. Large polymeric structures were sedimented by low speed centrifugation (10,000 × g) (Fig. 7*A*). In contrast to the other centrins, 70% of SdCen was sedimentable after the addition of Ca^{2+}. Only 14% of this precipitate was dissolved by washes with Ca^{2+} buffer. However, 57% of the precipitate was solubilized by EGTA, which specifically chelates Ca^{2+}. The remaining insoluble material was completely dissolved by SDS. Only a minor fraction of HsCen1 was sedimented (16%), which was then dissolved by Ca^{2+} and EGTA. For Cdc31p and HsCen2, hardly any precipitable material was obtained. None of the centrins sedimented with 10 mM Mg^{2+} (data not shown), indicating that the formation of polymers is specific for Ca^{2+}.

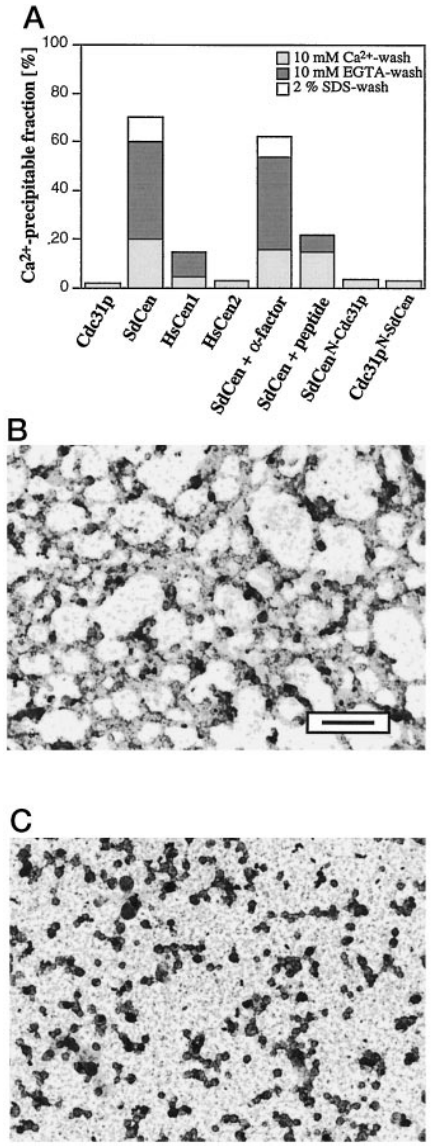

FIG. 7. **Ca^{2+}-dependent formation of SdCen polymers.** *A*, centrins were analyzed for their ability to form polymers at a protein concentration of 1.5 mM in the presence of 10 mM Ca^{2+}. In the experiment labeled *SdCen + α-factor*, α-factor was added before Ca^{2+} ions. In the experiment labeled *SdCen + peptide*, a synthetic peptide corresponding to the amino-terminal subdomain of SdCen (*underlined* in Fig. 1) was added before Ca^{2+}. The *bars* indicate the percentage of centrin that was sedimented by centrifugation (10,000 × g) after the addition of 10 mM Ca^{2+}. The sedimented material was washed with 10 mM Ca^{2+}, 10 mM EGTA, and 2% SDS. The marked areas represent the fractions of centrin that were solubilized under these washing conditions. The amount of protein in the different fractions is shown as a percentage of the total protein. *B*, shown is the filamentous network of SdCen. Induction of a filamentous network was performed by slowly increasing the Ca^{2+} concentration from 0 to 1 mM. SdCen filaments were analyzed by electron microscopy. *Bar* = 0.5 μm. *C*, the filamentous network in *B* was washed with 10 mM EGTA.

The amino-terminal extension of one SdCen molecule may interact with the peptide-binding site of another, thereby causing SdCen polymerization. We tested this hypothesis by exchanging the amino-terminal extension of Cdc31p with the corresponding sequence of SdCen ($Cdc31p^{N\text{-}SdCen}$) and vice versa ($SdCen^{N\text{-}Cdc31p}$). Interestingly, neither $Cdc31p^{N\text{-}SdCen}$ nor $SdCen^{N\text{-}Cdc31p}$ formed polymeric structures after the addition of Ca^{2+} (Fig. 7*A*). We also investigated whether Ca^{2+}-induced polymerization of SdCen was inhibited by a peptide corresponding to the amino-terminal subdomain of SdCen (Fig. 1,

Downloaded from http://www.jbc.org/ at Universitaetsbibliothek Medizin on November 16, 2017

underlined sequence), which is expected when the amino-terminal subdomain of SdCen interacts with another SdCen molecule. In agreement with our model, the SdCen peptide reduced SdCen polymerization by 65% (Fig. 7*A*, *SdCen + peptide*). If the amino-terminal subdomain of SdCen interacts with the same site as the Kar1p peptide, the latter should inhibit the polymerization reaction. As suggested by the results of Fig. 6, the addition of the Kar1p peptide inhibited SdCen polymerization by 80% (data not shown). Inhibition was specific for the SdCen and Kar1p peptides since similar concentrations of yeast α-factor hardly influenced SdCen polymerization (Fig. 7*A*, *SdCen + α-factor*).

We were interested in whether the polymerized form of SdCen consisted of filamentous structures. The polymerization reaction was induced by slowly increasing the Ca^{2+} concentration. SdCen polymers were then analyzed by electron microscopy. SdCen formed a network of filaments with a diameter of ~30 nm connected by crossing points of 50 nm (Fig. 7*B*). The connecting filaments were solubilized by EGTA, whereas the crossing points were resistant (Fig. 7*C*). Taken together, our findings are consistent with a model in which the amino-terminal subdomain of one SdCen molecule interacts with the peptide-binding site of another SdCen molecule, thereby causing the formation of a filamentous network.

Functional Analysis of Subdomains—Although all centrins bind with high affinity to the Cdc31p-binding site of Kar1p,[2] our biochemical analysis revealed differences in the polymerization behavior as well as in the Kar1p peptide-induced change in conformation. This raised the question whether centrins are interchangeable *in vivo*. SdCen was chosen for complementation studies in *S. cerevisiae* since it binds with similar affinity as Cdc31p to Kar1p[2] and extends like Cdc31p upon peptide binding (Fig. 4*B*).

Plasmid-encoded *SdCEN* and *CDC31* were under the control of the galactose-inducible *GAL1* promoter. Whether *GAL1-SdCEN* provides *CDC31* function was tested in strain ESM56, which carries the chromosomal *CDC31* gene under the control of the *MET3* promoter. Since the *MET3* promoter is repressed by methionine (42), ESM56 cells are unable to grow on methionine-containing medium unless *CDC31* function is replaced by *GAL1-SdCEN*. While ESM56 cells carrying *GAL1-CDC31* grew well on the methionine/galactose plates, *GAL1-SdCEN* cells did not grow, suggesting that *SdCEN* does not complement *CDC31*. We speculated that the polymerization of SdCen may be responsible for the noncomplementation. To test this possibility, $SdCEN^{N\text{-}CDC31}$ (SdCen with the amino-terminal subdomain from Cdc31p), which encodes for a hybrid protein that does not polymerize (Fig. 7*A*), was expressed in *MET3-CDC31* cells. As observed for *SdCEN*, $SdCEN^{N\text{-}CDC31}$ did not complement the *CDC31* depletion mutant either.

We exchanged each subdomain of Cdc31p with the corresponding domain of SdCen (the *arrows* in Fig. 1 indicate the fusion sites) in order to examine functional diversity. *CDC31-SdCEN* fusions, expressed from the *CDC31* promoter, were tested for *CDC31* function in strains ESM56 and ESM109. ESM109 has a disruption of the chromosomal *CDC31* gene and is kept alive by *CDC31* on a *URA3*-based plasmid. ESM109 cells do not grow on plates of 5-fluoroorotic acid, which selects against the *URA3* plasmid, unless *CDC31* function is provided on a separate *LEU2*-based plasmid. Since identical results were obtained with both strains, only those for ESM109 are shown (Fig. 8*A*). *CDC31* function was provided only by the $CDC31^{N\text{-}SdCEN}$ and $CDC31^{3\text{-}SdCEN}$ constructs (Fig. 8*A*, *sectors N* and *3*). We further noticed that $CDC31^{N\text{-}SdCEN}$ cells (Fig. 8*A*, *sector N*) grew slower in comparison with $CDC31^{3\text{-}SdCEN}$ (*sector 3*) and *CDC31* (*sector Cdc31p*) cells.

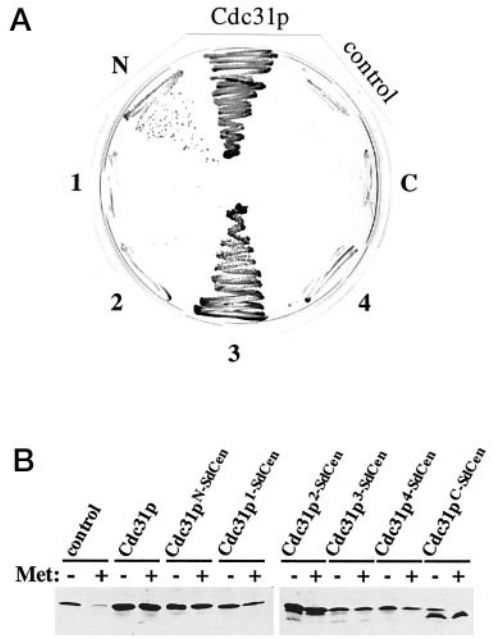

FIG. 8. ***SdCEN* does not fulfill *CDC31* functions.** *A*, ESM109 (Δ*cdc31::HIS3 CDC31* on a *URA3*-based plasmid) was transformed with the *LEU2*-based plasmid pRS425 (*sector control*) or with pRS425 carrying *CDC31* (*sector Cdc31p*), $CDC31^{N\text{-}SdCEN}$ (*sector N*), $CDC31^{1\text{-}SdCEN}$ (*sector 1*), $CDC31^{2\text{-}SdCEN}$ (*sector 2*), $CDC31^{3\text{-}SdCEN}$ (*sector 3*), $CDC31^{4\text{-}SdCEN}$ (*sector 4*), or $CDC31^{C\text{-}SdCEN}$ (*sector C*). Growth of the transformants was tested at 23 °C on 5-fluoroorotic acid plates. Growth on 5-fluoroorotic acid plates indicates that the plasmid-encoded *CDC31-SdCEN* gene fusion provided *CDC31* function. *B*, shown is the expression of *CDC31* and *CDC31-SdCEN* gene fusions. ESM56 contains the *CDC31* gene under the control of the *MET3* promoter. ESM56 cells with the control plasmid pRS426 (*control*) and with pRS426 carrying *CDC31*, $CDC31^{N\text{-}SdCEN}$, $CDC31^{1\text{-}SdCEN}$, $CDC31^{2\text{-}SdCEN}$, $CDC31^{3\text{-}SdCEN}$, $CDC31^{4\text{-}SdCEN}$, or $CDC31^{C\text{-}SdCEN}$ were incubated in medium with or without methionine. Cells extracts (80 μg of total protein) were then analyzed by immunoblotting with anti-Cdc31p antibodies. After 6 h in the repressing methionine medium, most of the *MET3-CDC31* was degraded (*control*, *+Met*). Therefore, the Cdc31p signal of *MET3-CDC31* cells grown in methionine medium (*+Met*) corresponds to the constitutively expressed, plasmid-encoded *CDC31* or *CDC31-SdCEN* gene.

An explanation for the noncomplementation of some *CDC31-SdCEN* constructs may be the instability of the fusion proteins. To test this possibility, the expression of *MET3-CDC31* of ESM56 was repressed by methionine. This allowed the detection of Cdc31p-SdCen proteins after degradation of Cdc31p. Most of the Cdc31p was degraded as indicated by ESM56 cells carrying the control plasmid or $CDC31^{C\text{-}SdCEN}$ (Fig. 8*B*). $Cdc31p^{C\text{-}SdCen}$ migrated differently than Cdc31p. The steady-state level of the Cdc31p-SdCen proteins was similar or higher in comparison with Cdc31p or functional $Cdc31p^{3\text{-}SdCen}$ (Fig. 8*B*).

The third EF-hand is the most conserved subdomain within the centrin family. Therefore, we investigated whether the third EF-hand of Cdc31p can be exchanged with the corresponding subdomain of ScCaM ($CDC31^{3\text{-}CMD1}$). Testing the functionality in ESM109 revealed that $CDC31^{3\text{-}CMD1}$ did not provide Cdc31p function (data not shown). In summary, our results suggest that Cdc31p is a specialized protein adapted to its specific functional requirements in *S. cerevisiae*.

DISCUSSION

We were interested in whether centrins involved in different cell functions have distinct biochemical properties. Cdc31p (centrosome duplication), SdCen (fiber contraction), HsCen1 and HsCen2 (unknown function), and ScCaM were purified

Downloaded from http://www.jbc.org/ at Universitaetsbibliothek Medizin on November 16, 2017

under identical conditions, and their biochemical properties were examined.

Apo State and Ca^{2+} Binding—So far, an α-helical value of 65% has been deduced from CD measurements only for CrCen (28). Since CrCen and SdCen are 91% identical, the 50% α-helical content of SdCen may be explained by the different methods applied for α-helical content calculation. Alternatively, CrCen may already form polymers at the protein concentrations used (0.5 or 5 mg/ml) in the CrCen CD measurements, although we ensured in our study that SdCen (0.1 mg/ml) and the other centrins were in their monomeric forms. Using CD spectroscopy, we could demonstrate that HsCen2 and SdCen did not change their overall α-helical content upon Ca^{2+} binding. This is no indication that Ca^{2+} binding does not alter the conformation of these centrins since Ca^{2+}-induced conformational changes were determined for CrCen by NMR (28) and for SdCen by size exclusion chromatography (Fig. 4*A*). In contrast to SdCen and HsCen2, Cdc31p showed a Ca^{2+}-induced increase in α-helical content, whereas for ScCaM and HsCen1, a decrease was observed. The 10% decrease in α-helical content of ScCaM was more pronounced than the 3% determined before (47).

The apo forms of the four centrins and ScCaM revealed an AMM ~1.7-fold higher than the calculated molecular mass. Since globular proteins were used for column calibration, this defined overestimation of the AMM suggests that centrins are likely to be elongated molecules perhaps with a domain architecture similar to calmodulin. Alterations in the AMM were observed upon Ca^{2+} addition and peptide binding, which most likely correspond to conformational changes in the proteins. We favor this interpretation since the changes in the AMM of ScCaM are in agreement with the conformational changes reported for vertebrate calmodulin (21, 22). In addition, the AMM alterations observed for centrins were the same at or below protein concentrations of 10 μM, making it unlikely that these AMM changes reflect an altered tendency of centrins to interact transiently. Finally, the AMM at 10 μM was minimally influenced by the ionic strength, excluding interactions with the gel matrix of the sizing column.

Holo Form and Peptide Binding—Ca^{2+} binding increased the AMM of ScCaM, while the AMM of centrins decreased, suggesting that centrins, in contrast to ScCaM, become more compact. The orientation of the EF-hands to each other and of the amino-terminal extension relative to the EF-hands may be responsible for the Ca^{2+}-induced behavior of centrins. Calmodulin shows a dumbbell-shaped molecule with two globular domains arranged in *trans* configuration connected by a central α-helix (22). It becomes more compact upon peptide binding, with the two globular domains facing each other in a *cis* orientation and the central helix disrupted by a flexible loop (22). Such a change to a more compact conformation may already occur in some centrins upon Ca^{2+} binding, explaining the strong Ca^{2+}-induced decrease in the AMMs of Cdc31p and SdCen (Fig. 4*A*). Alternatively, the long amino-terminal subdomain of centrins moves closer to the EF-hands, resulting in a more compact molecule. In any case, to understand the Ca^{2+}-induced conformational changes of centrins, high resolution structural studies are required.

The structure of calmodulin bound to the calmodulin-binding domain of skeletal muscle myosin light chain kinase has been solved. The extended structure of the holo form collapsed to a more compact molecule folded around the peptide (21). Similarly, ScCaM adopted a more compact conformation upon peptide binding (Fig. 4*B*). Also, the AMMs of the two human centrins decreased, suggesting that HsCen1 and HsCen2 bind to the target peptide in a similar manner as calmodulin. In contrast, the AMMs of Cdc31p and SdCen increased, which may be explained by a very compact conformation in the holo form, which expands to allow peptide binding.

Formation of a Centrin-based Filamentous Network—Centrins, but not ScCaM, formed multimers in the presence of Ca^{2+} and at protein concentrations above 10 μM. Under our *in vitro* conditions, Cdc31p had the lowest and SdCen had the highest tendency to form multimers (Fig. 6). Large polymeric structures of SdCen and HsCen1 were formed (SdCen, 70%; and HsCen1, 16%), which were sedimentable by low speed centrifugation (Fig. 7*A*). Since only large polymers sediment under this condition, we can not exclude that the other centrins form polymers that, however, are not as extended.

The formation of the SdCen polymers was dependent on the properties of the amino-terminal subdomain as well as the peptide-binding site. This conclusion is based on the following observations. Purified $SdCen^{N\text{-}Cdc31p}$ and $Cdc31p^{N\text{-}SdCen}$ fusion proteins did not form filaments, suggesting that neither the amino-terminal subdomain of SdCen nor the peptide-binding site is sufficient for the polymerization reaction (Fig. 7*A*). In addition, a synthetic peptide corresponding to the amino-terminal subdomain of SdCen inhibited the formation of SdCen filaments (Fig. 7*A*). Since also the Kar1p peptide reduced the formation of SdCen multimers (Fig. 6) and polymers, we favor a model in which the amino-terminal subdomain of one SdCen molecule interacts with the peptide-binding site of another, thereby forming a homodimer. A third SdCen molecule then interacts with either the free amino-terminal extension of the SdCen homodimer or the free peptide-binding site. Linear SdCen polymers may interact to form thicker filaments.

In flagellate green algae, centrin is the major protein of 4–8-nm filaments (53, 54). In contrast, our SdCen filaments were 30 nm thick, which may be the result of the artificial polymerization conditions. However, our results show for the first time that a purified centrin is able to form polymeric structures. Additional structural proteins and molecular chaperones may be required for the formation of filaments observed *in vivo*. Modifications of centrin, *e.g.* phosphorylation (54), could also influence filament formation.

The centrin-based fiber systems contract via a mechanism that involves filament supercoiling induced by Ca^{2+} binding to centrin (27). Consistent with a function in Ca^{2+}-dependent fiber contraction, SdCen showed the most pronounced changes in conformation upon Ca^{2+} binding (Fig. 4*A*). We assume that the SdCen subunits in the filaments behave in a similar way as the SdCen monomer. Since the SdCen subunits are likely connected via their amino-terminal subdomains, Ca^{2+}-induced contraction of each SdCen subunit will result in a rapid shortening of SdCen filaments.

Contribution of Subdomains to Function—It has been shown that *CrCEN* does not complement a temperature-sensitive allele of *CDC31* (55). In agreement with this result, SdCen did not replace Cdc31p function in yeast. However, Cdc31p hybrids with the amino-terminal subdomain or the third EF-hand from SdCen did (Fig. 8*A*). The functionality of $Cdc31p^{N\text{-}SdCen}$ was surprising since it had been suggested that the heterogeneous amino-terminal subdomains confer the functional diversity within centrins (17). However, $CDC31^{N\text{-}SdCEN}$ cells grew at a slower rate in comparison with *CDC31* cells (Fig. 8*A*), emphasizing the importance of the amino-terminal subdomain for centrin function. The third subdomain corresponds to one of the most conserved regions within centrins. Its importance in Cdc31p function was revealed by an exchange of the third EF-hand with the corresponding subdomain of ScCaM, resulting in an inactive hybrid protein. In contrast to centrins, the related calmodulins are less discriminative. Human (56) and

Downloaded from http://www.jbc.org/ at Universitaetsbibliothek Medizin on November 16, 2017

Schizosaccharomyces pombe (57) calmodulins support growth of *S. cerevisiae*. We suggest that centrins, in contrast to calmodulins, are proteins adapted to their specific functional requirements in each species.

In summary, centrins are most distinguishable from the calmodulin family by their ability to form multimeric structures. While SdCen clearly forms polymers *in vitro* and *in vivo* (58), it is not clear whether the other three centrins studied form polymeric structures *in vivo*. Human centrioles contract in response to the removal of divalent cations (59), a process that may involve centrin filaments. Cdc31p is associated with the half-bridge of SPB (29), which enlarges in the G_1 phase of the cell cycle (30). This may occur by Cdc31p polymerization.

Acknowledgments—We thank Drs. J. L. Salisbury and M. Bornens for providing *HsCEN1* and *HsCEN2*, respectively. Drs. M. Bornens and R. Arkowitz are gratefully acknowledged for reading the manuscript.

REFERENCES

1. Kalt, A., and Schliwa, M. (1993) *Trends Cell Biol.* **3,** 118–128
2. Kellogg, D. R., Moritz, M., and Alberts, B. M. (1994) *Annu. Rev. Biochem.* **63,** 639–674
3. Schiebel, E., and Bornens, M. (1995) *Trends Cell Biol.* **5,** 197–201
4. Oakley, C. E., and Oakley, B. R. (1989) *Nature* **338,** 662–664
5. Stearns, T., Evans, L., and Kirschner, M. (1991) *Cell* **65,** 825–836
6. Salisbury, J. L. (1995) *Curr. Opin. Cell Biol.* **7,** 39–45
7. Salisbury, J. L. (1989) *J. Phycol.* **25,** 201–206
8. Melkonian, M., Beech, P. L., Katsaros, C., and Schulze, D. (1992) in *Algal Cell Motility* (Melkonian, M., ed) pp. 179–221, Chapman and Hall Inc., New York
9. Zhu, J.-K., Bressan, R. A., and Hasegawa, P. M. (1992) *Plant Physiol.* (*Bethesda*) **99,** 1734–1735
10. Byers, B. (1981) *Alfred Benzon Symp.* **16,** 119–133
11. Baum, P., Furlong, C., and Byers, B. (1986) *Proc. Natl Acad. Sci. U. S. A.* **83,** 5512–5516
12. Lee, V. D., and Huang, B. (1993) *Proc. Natl Acad. Sci. U. S. A.* **90,** 11039–11043
13. Errabolu, R., Sanders, M. A., and Salisbury, J. L. (1994) *J. Cell Sci.* **107,** 9–16
14. Kawasaki, H., and Kretsinger, R. H. (1995) *Protein Profile* **2,** 297–490
15. Huang, B., Watterson, D. M., Lee, V. D., and Schibler, M. J. (1988) *J. Cell Biol.* **107,** 121–131
16. Moncrief, N. D., Kretsinger, R. H., and Goodman, M. (1990) *J. Mol. Evol.* **30,** 522–562
17. Bhattacharya, D., Steinkötter, J., and Melkonian, M. (1993) *Plant Mol. Biol.* **23,** 1243–1254
18. Schiebel, E., Driessen, A. J. M., Hartl, F.-U., and Wickner, W. (1991) *Cell* **64,** 927–939
19. Vogel, H. J. (1994) *Biochem. Cell Biol.* **72,** 357–376
20. Babu, Y. S., Sack, J. S., Greenhough, T. J., Means, A. R., and Cook, W. J. (1985) *Nature* **315,** 37–40
21. Ikura, M., Clore, G. M., Gronenborn, A. M., Zhu, G., Klee, C. B., and Bax, A. (1992) *Science* **256,** 632–638
22. Barbato, G., Ikura, M., Kay, L. E., Pastor, R. W., and Bax, A. (1992) *Biochemistry* **31,** 5269–5278
23. Wright, R. L., Salisbury, J., and Jarvik, J. W. (1985) *J. Cell Biol.* **101,** 1903–1912
24. McFadden, G. I., Schulze, D., Surek, B., Salisbury, J. L., and Melkonian, M. (1987) *J. Cell Biol.* **105,** 903–912
25. Baron, A. T., and Salisbury, J. L. (1988) *J. Cell Biol.* **107,** 2669–2678
26. Sanders, M. A., and Salisbury, J. L. (1994) *J. Cell Biol.* **124,** 795–805
27. Salisbury, J. L. (1983) *J. Submicrosc. Cytol.* **15,** 105–110
28. Weber, C., Lee, V. D., Chazin, W. J., and Huang, B. (1994) *J. Biol. Chem.* **269,** 15795–15802
29. Spang, A., Courtney, I., Fackler, U., Matzner, M., and Schiebel, E. (1993) *J. Cell Biol.* **123,** 405–416
30. Byers, B. (1981) in *The Molecular Biology of the Yeast Saccharomyces: Life Cycle and Inheritance* (Strathern, J. N., Jones, E. W., and Broach, J. R., eds) pp. 59–96, Cold Spring Harbor Laboratory, Cold Spring Harbor, NY
31. Biggins, S., and Rose, M. D. (1994) *J. Cell Biol.* **125,** 843–852
32. Spang, A., Courtney, I., Grein, K., Matzner, M., and Schiebel, E. (1995) *J. Cell Biol.* **128,** 863–877
33. Vallen, E. A., Ho, W., Winey, M., and Rose, M. D. (1994) *Genetics* **137,** 407–422
34. Guthrie, C., and Fink, G. R. (1991) *Methods Enzymol.* **194,** 12–17
35. Schiestl, R. H., and Gietz, R. D. (1989) *Curr. Genet.* **16,** 339–346
36. Dower, W. J., Miller, J. F., and Ragsdale, C. W. (1988) *Nucleic Acids Res.* **16,** 127–145
37. Sanger, F., Nicklen, S., and Coulson, A. R. (1977) *Proc. Natl. Acad. Sci. U. S. A.* **74,** 5463–5467
38. Sambrook, J., Fritsch, E. F., and Maniatis, T. (1989) *Molecular Cloning: A Laboratory Manual*, Cold Spring Harbor Laboratory, Cold Spring Harbor, NY
39. Davis, T. N., Urdea, M. S., Masiarz, F. R., and Thorner, J. (1986) *Cell* **47,** 423–431
40. Tabor, S., and Richardson, C. C. (1985) *Proc. Natl. Acad. Sci. U. S. A.* **82,** 1074–1078
41. Christianson, T. W., Sikorski, R. S., Dante, M., Shero, J. H., and Hieter, P. (1992) *Gene* (*Amst.*) **110,** 119–122
42. Mountain, H. A., Byström, A. S., Larsen, J. T., and Korch, C. (1991) *Yeast* **7,** 781–803
43. Ausubel, F. M., Brent, R., Kingston, R. E., Moore, D. D., Seidman, J. G., Smith, J. A., and Struhl, K. (eds) (1994) *Current Protocols in Molecular Biology*, John Wiley & Sons, Inc., New York
44. Sandermann, H., Jr., and Strominger, J. (1972) *J. Biol. Chem.* **247,** 5123–5131
45. Bradford, M. M. (1976) *Anal. Biochem.* **72,** 248–254
46. Provencher, S. W., and Glockner, J. (1981) *Biochemistry* **20,** 33–37
47. Ohya, Y., Uno, I., Ishikawa, T., and Anraku, Y. (1987) *Eur. J. Biochem.* **168,** 13–19
48. Baron, A. T., Errabolu, R., Dinusson, J., and Salisbury, J. L. (1995) *Methods Cell Biol.* **47,** 341–351
49. Travé, G., Lacombe, P.-J., Pfuhl, M., Saraste, M., and Pastore, A. (1995) *EMBO J.* **14,** 4922–4931
50. Stirling, D. A., Welch, K. A., and Stark, M. J. R. (1994) *EMBO J.* **13,** 4329–4342
51. Geiser, J. R., Sundberg, H. A., Chang, B. H., Muller, E. G. D., and Davis, T. N. (1993) *Mol. Cell. Biol.* **13,** 7913–7924
52. Salisbury, J. L., Sanders, M. A., and Harpst, L. (1987) *J. Cell Biol.* **105,** 1799–1805
53. Baron, A. T., and Salisbury, J. L. (1992) in *The Centrosome* (Kalnins, V. I., ed) pp. 167–195, Academic Press, Inc., San Diego, CA
54. Salisbury, J. L., Baron, A., Surek, B., and Melkonian, M. (1984) *J. Cell Biol.* **99,** 962–970
55. Lee, V. D., and Huang, B. (1990) in *Calcium as an Intracellular Messenger in Eucaryotic Microbes* (O'Day, D. H., ed) pp. 245–257, American Society for Microbiology, Washington, D. C.
56. Davis, T. N., and Thorner, J. (1989) *Proc. Natl. Acad. Sci. U. S. A.* **86,** 7909–7913
57. Moser, M. J., Lee, S. Y., Klevit, R. E., and Davis, T. N. (1995) *J. Biol. Chem.* **270,** 20643–20652
58. Schulze, D., Robenek, H., McFadden, G. I., and Melkonian, M. (1987) *Eur. J. Cell Biol.* **45,** 51–61
59. Paintrand, M., Moudjou, M., Delacroix, H., and Bornens, M. (1992) *J. Struct. Biol.* **108,** 107–128
60. Spang, A., Grein, K., and Schiebel, E. (1996) *J. Cell Sci.*, in press

Downloaded from http://www.jbc.org/ at Universitaetsbibliothek Medizin on November 16, 2017

Characterization of Green Alga, Yeast, and Human Centrins: SPECIFIC SUBDOMAIN FEATURES DETERMINE FUNCTIONAL DIVERSITY

Hans Wiech, Birgitta M. Geier, Thilo Paschke, Anne Spang, Katrin Grein, Jutta Steinkötter, Michael Melkonian and Elmar Schiebel

J. Biol. Chem. 1996, 271:22453-22461.
doi: 10.1074/jbc.271.37.22453

Access the most updated version of this article at http://www.jbc.org/content/271/37/22453

Alerts:
- When this article is cited
- When a correction for this article is posted

Click here to choose from all of JBC's e-mail alerts

This article cites 53 references, 23 of which can be accessed free at
http://www.jbc.org/content/271/37/22453.full.html#ref-list-1

Downloaded from http://www.jbc.org/ at Universitaetsbibliothek Medizin on November 16, 2017